Transactions, SMiRT-26
Berlin/Potsdam, Germany, July 10-15, 2022
Division V

A STUDY ON THE IMPROVEMENT OF ACCURACY OF THREE-DIMENSIONAL SEISMIC EVALUATION ANALYSIS METHOD FOR NUCLEAR BUILDINGS USING A LARGE-SCALE OBSERVATION SYSTEM

Akemi Nishida[1], Manabu Kawata[2], Byunghyun Choi[3], Kazuhiko Iigaki[4] and Yinsheng Li[5]

[1] Deputy Division Head, Japan Atomic Energy Agency, Ibaraki, Japan (nishida.akemi@jaea.go.jp)
[2] Assistant Principal Engineer, Japan Atomic Energy Agency, Ibaraki, Japan
[3] Assistant Principal Researcher, Japan Atomic Energy Agency, Ibaraki, Japan
[4] Manager, Japan Atomic Energy Agency, Ibaraki, Japan
[5] Division Head, Japan Atomic Energy Agency, Ibaraki, Japan

ABSTRACT

Our research and development were aimed at improving the accuracy of the three-dimensional seismic evaluation analysis method for nuclear buildings that contributes to the probabilistic risk assessment caused by earthquakes (seismic PRA). In 2019, we began our research on improving the accuracy and validating the three-dimensional seismic analysis method for nuclear buildings using actual seismic observation records in collaboration with the Nuclear Regulation Authority (NRA). In this study, we constructed a large-scale observation system that enabled simultaneous measurements at multiple positions during earthquakes or using artificial waves. The accelerometers of the observation system were installed not only on/in the soil and on the floors, but also on the walls of the building. Here, we report an outline of the large-scale observation system and the knowledge obtained from the analysis results of the seismic observation records acquired using the system.

INTRODUCTION

In Japan, new regulatory requirements have strengthened the safety evaluation caused by natural disasters, such as earthquakes, and the 2013 operational guide for safety improvement evaluation recommends the use of a probabilistic risk assessment (PRA) as an evaluation method. Important issues in the seismic PRA are the realistic assessment of structural seismic response including local response and local damage for the evaluation of damage probability (fragility) of nuclear facilities. For the purpose, it is expected to utilize the three-dimensional seismic evaluation analysis method for nuclear buildings that can express the local response of the floor and wall where important equipment is installed.

In recent years, the seismic evaluation analysis methods using a three-dimensional finite element model has been used to evaluate the seismic responses of reactor buildings (for example, Nakamura, et al. (2008)). To validate this method, it was necessary to confirm the consistency of the analytical results with the observation records. In a study on the three-dimensional seismic evaluation analysis method of reactor buildings, a benchmark analysis comparing the analytical results and observation records during the Niigataken Chuetsu-oki Earthquake in 2007 at the Kashiwazaki-Kariwa Nuclear Power Plant was conducted by the International Atomic Energy Agency (IAEA (2013)). These studies revealed that there are problems with the variability of results by analysts or organizations and the reproducibility of observation records.

Against this background, authors have confirmed the influence of important factors related to the three-dimensional seismic evaluation analysis method on the building response, and have been working on

standardization of the analysis procedures, method, etc. that contribute to improving the accuracy of three-dimensional seismic evaluation analysis methods. In addition, in order to further improve the accuracy of the three-dimensional seismic evaluation analysis method, it is necessary to confirm the validity of the method by comparing it with seismic observation records including local responses such as floors and walls. Issues for that purpose are lacks of detailed information on the target structure, detailed observation records on floors and walls, and the number of earthquakes. Therefore, in this research, we dealt with these issues as follows;

- By targeting the facilities in the Japan Atomic Energy Agency, detailed information on the structure can be obtained,
- By installing the accelerometer not only on the floor but also on the wall, simultaneous observation at multiple points is realized, and
- By combining earthquakes and artificial waves, necessary data can be obtained. In addition, by combining artificial waves and mobile accelerometers, observations at arbitrary positions on floors and walls are possible.

Therefore, in this study, we installed a large number of accelerometers on the floor and walls of the High Temperature Engineering Test Reactor (HTTR) building (hereinafter referred to as "HTTR building") of the Japan Atomic Energy Agency, where detailed plant information can be obtained, to construct a large-scale observation system. This system can observe not only earthquakes but also artificial waves, and work on the improvement of the three-dimensional seismic evaluation analysis method of the building. This research was carried out in collaboration with the Nuclear Regulatory Authority and the Japan Atomic Energy Agency.

In this paper, initially, we will give an overview of the large-scale observation system constructed in the HTTR building. Next, observation records of earthquakes and artificial waves obtained using the large-scale observation system, and the vibration characteristics such as the predominant frequency and corresponding vibration mode of the building analyzed using the actual measurement data are shown. Finally, a three-dimensional analysis model based on the finite element method for the HTTR building was prepared and improved by reflecting the obtained vibration characteristics, and the validity of the three-dimensional evaluation analysis method was considered by comparing the seismic observation records with the analysis results.

CONSTRUCTION OF A LARGE-SCALE OBSERVATION SYSTEM

Outline of the HTTR Building

The main structure of the HTTR building, which is the target building, is a reinforced concrete structure (partly SRC or S structure) with a steel-framed flat roof. The plan size of the building is 52.0 m (NS) x 50.0 m (EW), which is almost a square, and it has three basement floors and two floors above the ground. The foundation slab is a solid foundation with a thickness of 5.0 m and is installed directly in the Ishizaki Formation of the Quaternary Formation, which is the supporting ground. Figure 1 presents an overview of the HTTR building.

Overview of the Large-Scale Observation System

We installed a large number of accelerometers on the floor and walls of the HTTR building of the Japan Atomic Energy Agency. Here, detailed plant information can be obtained to construct a large-scale observation system that can observe not only earthquakes but also artificial waves, and also work on improving the three-dimensional seismic analysis method of the building. Figure 2 presents an overview of the large-scale observation system.

Figure 1. Overview of HTTR

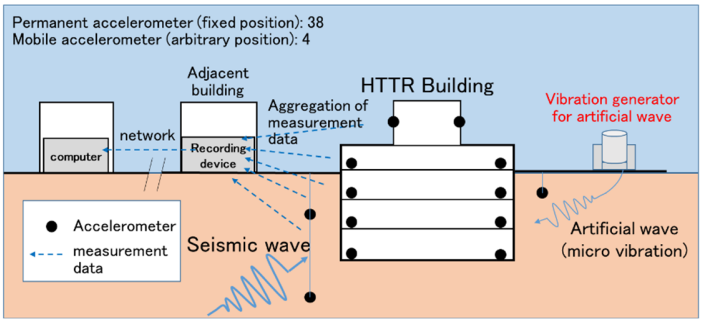

Figure 2. Overview of the large-scale observation system

Development of an Observation System for Earthquakes

Figure 3 shows the layout of the accelerometers installed in the HTTR building and the surrounding ground. The accelerometers indicated by ● were installed in 1997 at 12 locations, mainly on the basement floor, and in nine other locations on the ground (Ebisawa, et al. (2001)). In this study, we focused on the above-ground floors where only a few accelerometers were installed to measure the response of the entire building in detail. A total of 17 accelerometers (N1–N3, S1–S2, W1–W3, and E1–E3 in Fig. 3) were installed along the exterior walls of the building (Fig. 4 (a)). The installation height was set at the floor position of each floor. Figure 4 (b) shows the installation status of the accelerometer installed on the ground surface. In addition to the permanent accelerometers, four portable mobile accelerometers (Fig. 4 (c)) were prepared. With the addition of mobile accelerometers, any position or a position where it is difficult to install a permanent accelerometer can be measured, for example, the center of the floor or around the opening. Since March 2020 when the large-scale observation system was installed, we have experienced a total of over 50 earthquakes with a seismic intensity of one or higher and have obtained observation records.

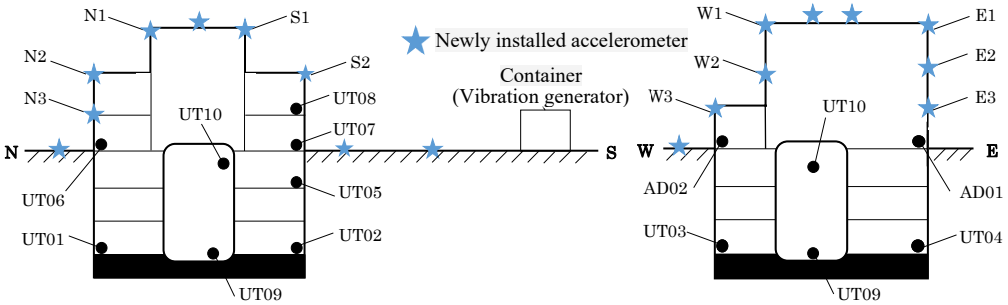

(a) North-South (NS) direction (b) East-West (EW) direction

Figure 3. Permanent accelerometer installation position

(a) Accelerometer on exterior walls (b) Ground Accelerometer (c) Mobile Accelerometer

Figure 4. Installation of the accelerometers

Development of an Observation System using Artificial Waves

ACROSS (Kumazawa, et al. (2003)) was introduced as an observation system capable of transmitting artificial waves at a point 35 m south of the HTTR building approximately (Fig. 5). ACROSS in this research consists of a vibration generator that generates vibrations by swinging the weight up and down, and a control device to control the vibrations. The control device drives both, the vibration generator based on the transmission signal, and the mechanism that transmits the vibrations to the HTTR building by vibrating the ground through the reinforced concrete (RC) foundation under the vibration generator installed in the container, as shown in Fig. 5.

Figure 6 shows an example of the transmission signals of an artificial wave. In addition, Fig. 7 shows an example of the acceleration time-history waveform measured at the building basemat for the signal shown in Fig. 6. The transmitted signal is generated by the superposition of standing waves in the frequency range of 3 to 30 Hz, with frequency increments of 0.5 Hz. The frequency range and interval of the transmitted signals can be set arbitrarily. So far, we have conducted a total of 40 observations using the ACROSS and have obtained observation records at about 90 positions.

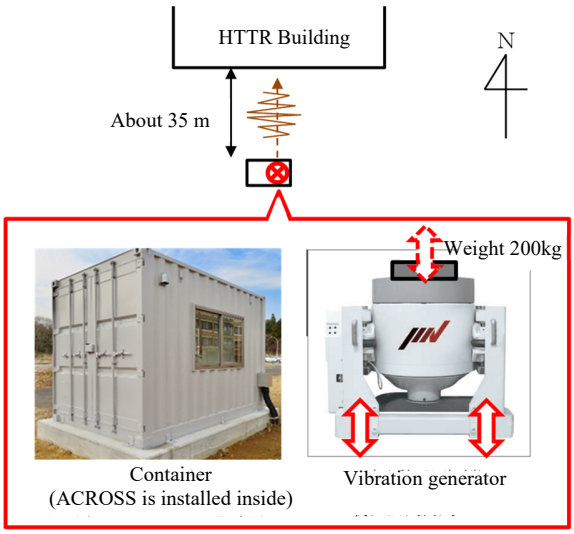

Figure 5. Overview of ACROSS

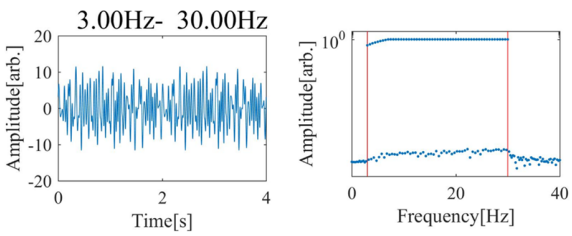

(a) Waveform of time history (b) Fourier spectrum

Figure 6. An example of signals of an artificial wave

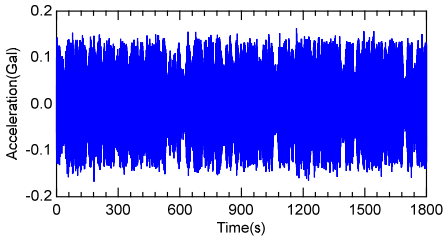

Figure 7. Acceleration time history measured on the building basemat (UT02, Up-Down (UD) direction)

ANALYSIS OF THE VIBRATION CHARACTERISTICS OF THE BUILDING

Analysis using the Acceleration Response Excited by an Earthquake

Table 1 lists the target seismic observation records presented in this study. There were five such records of seismic intensity three observed in Oarai Town in 2020. As an example of the analysis results of the predominant frequency, Fig. 8 (a) shows the results of the Fourier amplitude ratio of the rooftop (S1) to the basemat (UT02) on the south side of the building using the four earthquakes in Table 1. It shows almost the same characteristics for all seismic motions, such as the peak frequency. In addition, the earthquake on February 13, 2021, was excerpted from the four earthquakes, and the Fourier amplitude ratios of the roof (S1), third floor (S2), second floor (UT08), first floor (UT07), and the first basement floor (UT05) with respect to the basemat (UT02) on the south side of the building are shown in Fig. 8 (b). Also, the peak frequencies around 4 Hz, 7 Hz, and 10 Hz (● in the figure), which are considered the predominant frequencies corresponding to the main vibration characteristics, were confirmed from Fig. 8 (b). This result is similar to those of previous studies in references Nishida, et al. (2020) and Yamakawa, et al. (2020).

Table 1: The target seismic observation records

Observation records information		Epicenter depth	Magnitude	Earthquake intensity at Oarai-machi
Date	Epicenter			
12 April, 2020	Southern Ibaraki Prefecture	53 km	5.0	3
22 November, 2020	Offshore Ibaraki prefecture	45 km	5.7	3
30 December, 2020	Offshore Ibaraki prefecture	56 km	5.2	3
13 February, 2021	Offshore Fukushima Prefecture	55 km	7.3	3

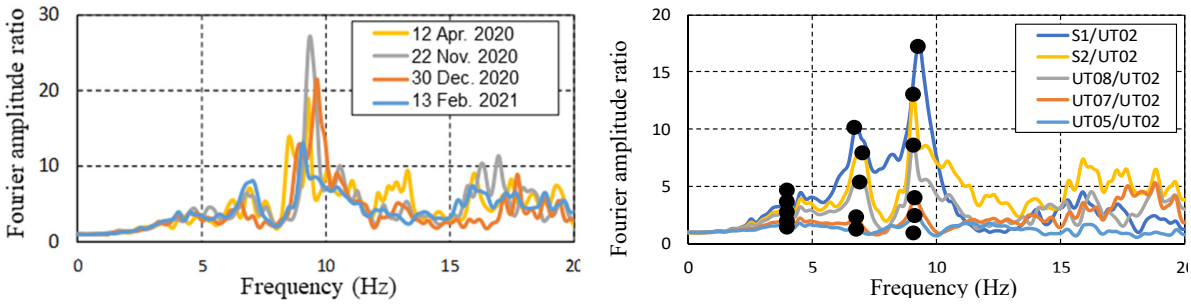

(a) S1/UT02, NS direction (b) NS direction

Figure 8. Fourier amplitude ratio (Earthquake occurred on February 13, 2021)

Figure 9 shows the results of the deformation mode of the entire building for the dominant frequencies of 4 Hz, 7 Hz, and 10 Hz, as confirmed in Section 3.1.2. From Fig. 9, it can be observed that the vibration characteristics of the building are different at each predominant frequency. Multiple modes were observed at a predominant frequency of approximately 4 Hz. It can be confirmed that each floor of the building was tilted, the entire building rotated, and the building appeared twisted. On the other hand, at predominant frequencies of approximately 7 Hz and 10 Hz, the rotational displacement of the basement hardly occurred, and the deformation of the building itself was dominant. Furthermore, it was confirmed that the north and south outer walls vibrate in the same direction at a frequency of approximately 7 Hz, whereas they vibrate in the opposite direction at a frequency of approximately 10 Hz.

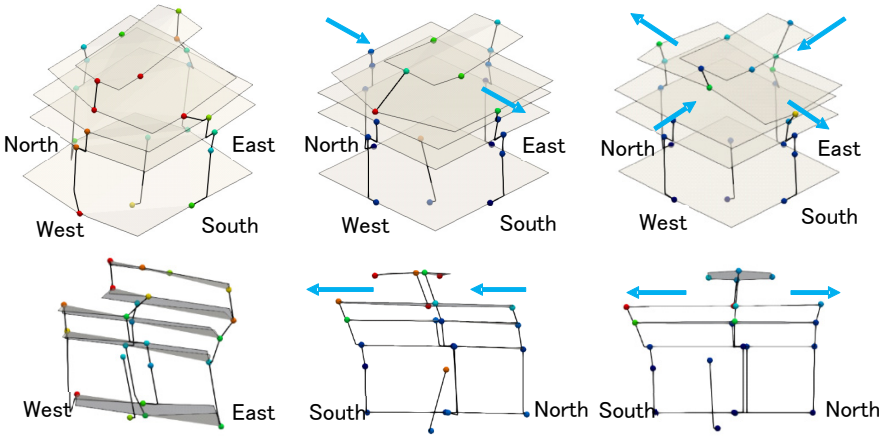

(a) Around 4Hz (b) Around 7Hz (c) Around 10Hz

Figure 9. Examples of building deformation mode (the earthquake occurred on February 13, 2021)

Analysis using the Acceleration Response Excited by the Transmission Signal of Artificial Waves

Figure 10 shows the placement position of the mobile accelerometer used for the observation of artificial waves using ACROSS. The three mobile accelerometers were placed in a straight line on the floor of the second floor on the south side of the building to measure the floor's local response. It has a few earthquake-resistant walls on the lower floor, The transmitted signal was created by superimposing standing waves with frequencies of 3–30 Hz (0.5 Hz intervals), as shown in Fig. 11.

As in the case of seismic observation records, the Fourier amplitude ratio and deformation mode were calculated, and the local vibration characteristics of the floor were analyzed. Figures 12 (a) and 12 (b) show examples of the results of calculating the Fourier amplitude ratio of the mobile accelerometers M3 and M4 in the UD direction with respect to the mobile accelerometer M2 placed on the earthquake-resistant wall on the second floor of the building, respectively. From the Fourier amplitude ratio, it can be observed that the floor to be analyzed has a predominant frequency of approximately 17.5 Hz in the UD direction. In addition, it is estimated that the deformation mode from the amplitude ratios of the mobile accelerometers M3 and M4 to the mobile accelerometer M2 at 17.5 Hz is as shown in Fig. 13.

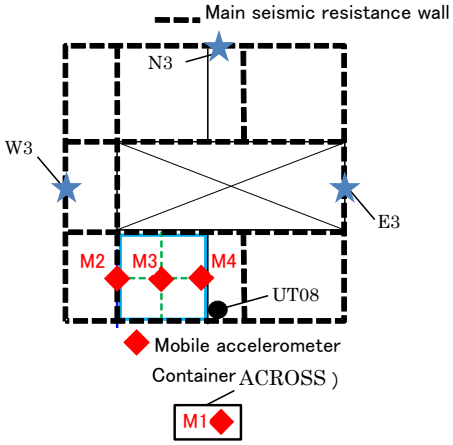

Figure 10. An example of mobile accelerometer placement (2nd floor of the building)

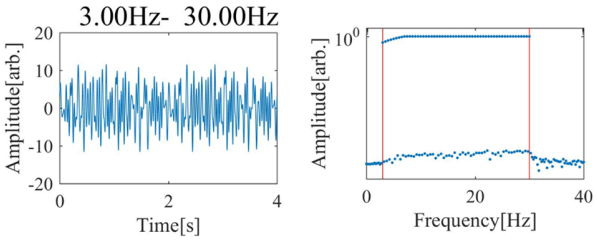

(a) Time-history waveform (b) Fourier amplitude

Figure 11. An example of the transmission signal of an artificial wave using ACROSS

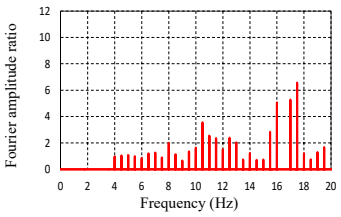

(a) M3 / M2, UD direction

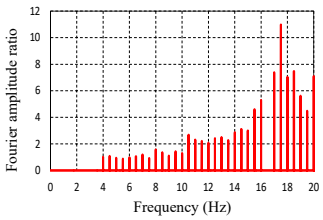

(b) M4 / M2, UD direction

Figure 12. Fourier amplitude ratio

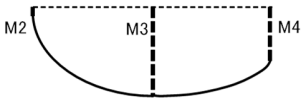

Figure 13. Local deformation mode of the target local floor

ANALYSIS USING A THREE-DIMENSIONAL FINITE ELEMENT MODEL

Three-Dimensional Finite Element Model (3D FEM Model) of the Building

As 3D FEM models of the building, a shell element model (number of nodes: 239,076; number of elements: 237,625) and a solid element model (number of nodes: 421,657; number of elements: 1,420,725) were prepared (Fig. 14). In the shell element model, a shell, beam, and solid elements were used for the main structure, roof truss, and basemat, respectively. The soil structure was modeled using solid elements to enable simultaneous inputs in three directions. On the other hand, the building and soil of the solid element model were modeled using tetrahedral primary elements. The roof truss and containment vessel were modeled using beam and shell elements, respectively.

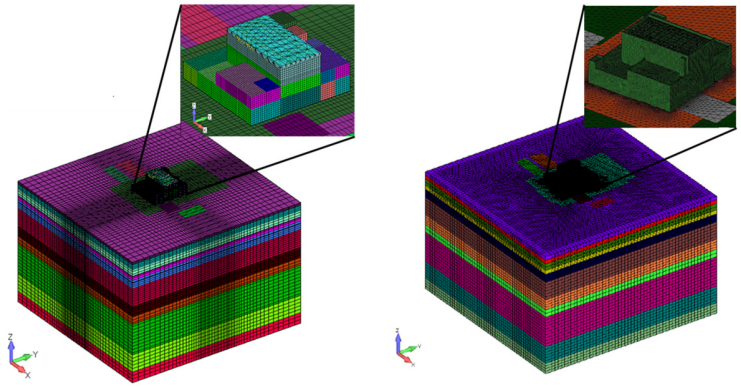

(a) Shell element model (b) Solid element model.

Figure 14. Three-dimensional FEM Model

Tables 2 and 3 show the soil and building material properties of the 3D FEM model, respectively. The soil properties are the convergent values obtained by performing an equivalent linear analysis for each seismic motion. Table 2 shows the soil properties set based on the seismic observation records of April 12, 2020. For the boundary of the side surface of the soil, the periodic boundary condition was set such that the soil nodes facing each other at the same height on opposite sides had the same displacement, and the boundary of the bottom of the soil structure was modeled with the damper. From the previous studies Nishida, et al (2015), the boundary condition between the soil and the building was assumed to be free from G.L.0.0 m to G.L.-3.3 m, and a rigid connection from G.L.-3.3 m to the bottom of the soil structure.

Table 2: Examples of soil properties of the shell element model
(Based on the earthquake observation record on April 12, 2020)

Geological layer	Depth GL(m)	Layer thickness (m)	Ground parameters					
			Mass density γ (tf/m^3)	Shear wave velocity V_s (m/s)	Primary wave velocity V_p(m/s)	Shear modulus G (N/m^2)	Poisson's ratio	Transmission frequency f_{max}(Hz)
Loam	0.0	3.5	1.33	230	850	7.04E+07	0.46	35.38
Miwa	3.5	4.5	1.93	350	980	2.36E+08	0.43	31.96
	8.0	1.5	1.78	300	970	1.60E+08	0.45	40.00
	9.5	11.0	1.82	440	1100	3.52E+08	0.41	22.86
	20.5	6.0	2.05	650	1300	8.66E+08	0.33	43.33
Ishizaki	26.5	12.0	1.93	430	1590	3.57E+08	0.46	28.67
	38.5	1.5	1.89	380	1580	2.73E+08	0.47	50.67
	40.0	24.5	1.85	370	1580	2.53E+08	0.47	24.16
	64.5	15.0	1.87	390	1580	2.84E+08	0.47	20.80
	79.5	11.0	2.02	490	1680	4.85E+08	0.45	21.78
Pliocene	90.5	44.0	1.79	480	1630	4.12E+08	0.45	20.04
	134.5	25.0	1.82	540	1680	5.31E+08	0.44	21.60
	159.5	15.5	1.86	590	1730	6.47E+08	0.43	23.60
Miocene	175.0	-	1.99	1020	2170	2.07E+09	0.36	-

Table 3: Material properties of the shell element model

Part	Unit weight γ (kN/m^3)	Young's modulus E (kN/m^2)	Shear modulus G (kN/m^2)	Poisson's ratio	Damping ratio h (%)
R/B, I/C	24	2.25E+07	9.38E+06	0.2	3.0
C/V	77	1.89E+08	7.28E+07	0.3	1.0
Truss	77	2.05E+08	7.88E+07	0.3	2.0

Analysis Result of Eigenvalue analysis

To understand the vibration characteristics of the 3D FEM model, its natural frequency and natural mode were obtained by eigenvalue analysis (Table 4, Fig. 15, and Fig. 16). The natural frequency obtained from the eigenvalue analysis is compared to the predominant frequencies of the building (approximately 4 Hz, 7 Hz, and 10 Hz) obtained from the seismic observation record (shown in Section 3.1). The second-order natural frequency is on the low-frequency side, and the third-order natural frequency is on the high-frequency side in both the shell and solid element models; however, the results are generally the same. Regarding the unique mode, almost the same result as that of the deformation mode diagram got from the seismic observation record was obtained.

Table 4: List of natural frequencies of the 3D FEM models

	NS			EW		
	1st (Hz)	2nd (Hz)	3rd (Hz)	1st (Hz)	2nd (Hz)	3rd (Hz)
Shell element model	3.20	5.72	11.84	3.16	6.48	12.84
Solid element model	3.94	7.11	10.94	3.93	7.26	11.50

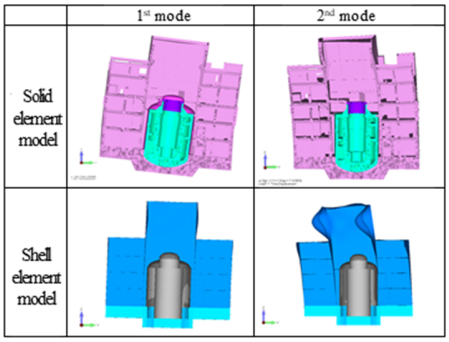

Figure 15. Examples of natural modes (primary and secondary modes, NS direction)

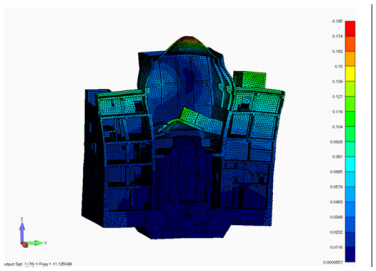

Figure 16. An example of natural mode (the solid element model, NS direction)

Analytical Results of Frequency Response Analysis

Figure 17 shows the comparison results between the Fourier amplitude ratios of the shell element and solid element model obtained by frequency response analysis, and the Fourier amplitude ratios obtained from seismic observation records. Compared to the seismic observation record, the analytical results show that the peak frequency is uniformly shifted to the high frequency side for the solid element model. The rigidity of the tetrahedral primary element used as a component of the solid element model is evaluated to be slightly stiffer than the actual stiffness. Using the tetrahedral quadratic element is expected to solve the above problems, and we confirmed the effect through preliminary analysis.

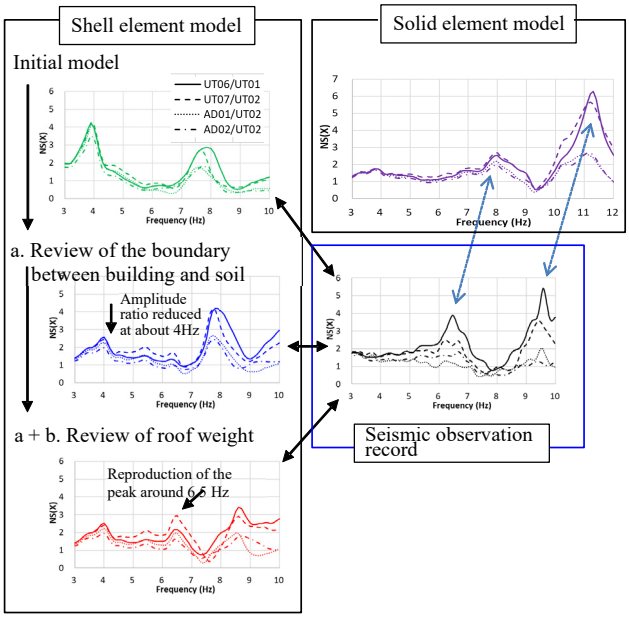

Figure 17. Comparison of analytical results and seismic observation records (Fourier amplitude ratio)

In contrast, in the initial model, the shell element model showed a different property compared to the seismic observation record in terms of the Fourier amplitude ratio. Therefore, the model was reviewed using the information related to design and construction. In particular, by reviewing the rigidity of the artificial rock (MMR) at the boundary between the building and the soil, its difference from that of the observation record was improved. As a result, the response amplification near 4 Hz was reduced, which is related to the rotational motion of the building. Furthermore, we reviewed on ways to set the weight of the

3D FEM model. Conventionally, on each floor, the mass of the 3D FEM model is set to be equivalent to the mass of the Sway-Rocking (SR) model. First, we reviewed the mass of the roof, which had almost no load weight upon it. As a result, the excitation of the predominant frequency around 6.5 Hz, which is a characteristic vibration around the roof and the operation floor was observed, and the result consistent with the observation record was obtained. Because it was confirmed that the modeling of the mass distribution is highly sensitive to the building response, the distribution of the load weight on other floors will be reviewed in the future. We plan to further improve upon the model by considering the modeling method of the non earthquake-resistance members, setting the analysis target range and so on.

SUMMARY

We constructed a large-scale observation system that can observe earthquakes and artificial waves at the HTTR building of the Japan Atomic Energy Agency. The system can observe the entire as well as local responses of the building. The vibration characteristics of the entire building were analyzed using seismic observation records. In addition, the vibration characteristics of the local floors and walls of the building were analyzed using measured data obtained from artificial waves in the large-scale observation system.

Moreover, we prepared three-dimensional FEM models of the building and compared the analysis results with the seismic observation records through eigenvalue analysis and frequency response analysis. We also examined the important factors and settings of the modeling method related to the vibration characteristics of the building. In addition, the 3D FEM model was modified to improve the reproducibility of the seismic observation records by comparing it with the analytical result.

In the future, we will proceed with the acquisition and analysis of more diverse data to improve the three-dimensional seismic evaluation analysis method and work to solve the problems of the method. We plan to confirm the validity of the three-dimensional seismic evaluation analysis method continuously.

ACKNOWLEDGMENTS

This research was conducted as the joint research between the Nuclear Regulation Authority and the Japan Atomic Energy Agency, using actual plant data and actual measurement data of the HTTR of the Oarai Research Institute of the Japan Atomic Energy Agency. We would like to express our sincere gratitude to all the people concerned for their cooperation.

REFERENCES

Choi, B., et al. (2022), “Standard Guideline for the Seismic Response Analysis Method Using 3D Finite Element Model of Reactor Buildings”, JAEA-Research 2021-017. (in Japanese)

Ebisawa, K., et al. (2001), “Earthquake Observation Database in JAERI Oarai Site obtained by Vertical Instrument Arrays from 1987~2000”, JAERI -Data/Code 2001 -009. (in Japanese)

IAEA (2013), “Review of Seismic Evaluation Methodologies for Nuclear Power Plants Based on a Benchmark Exercise", IAEA-TECDOC-1722.

Kumazawa, M., et al. (2007), “Development of ACROSS (Accurately Controlled, Routinely Operated, Signal System) to realize constant monitoring the invisible Earth’s interiors by means of stationary coherent elastic and electromagnetic waves”, JAEA-research, 2007-033. (in Japanese)

Nakamura, N., et al. (2008), “Response Behavior of Nuclear Power Plant Building for Simultaneous Horizontal and Vertical Motions using 3D FEM Model Considering Basemat Uplift”, Journal of Structural Engineering, Vol.54B, pp.581-589. (in Japanese)

Nishida, A., et al. (2015), “Seismic response simulation of High-Temperature Engineering Test Reactor building against 2011 Tohoku earthquake”, Proceedings of 23rd International Conference on Nuclear Engineering (ICONE-23), 7 pages.

Nishida, A., et al. (2020), “Estimation of Vibration Characteristics of Nuclear Facilities by Analyzing Earthquake Observation Records (Part 1: Analysis Method)”, Summaries of technical papers of annual meeting, Architectural Institute of Japan, pp. 1105-1106. (in Japanese)

Yamakawa, K., et al. (2020), “Estimating the vibration characteristics of nuclear facilities from seismic observation records (Part 2: Analysis results)”, Summaries of technical papers of annual meeting, Architectural Institute of Japan, pp. 1107-1108. (in Japanese)